AJNR

CT findings in spinocerebellar degeneration.

A Ramos, F Quintana, C Díez, C Leno and J Berciano

This information is current as of April 26, 2024.

CT Findings in Spinocerebellar Degeneration

Ana Ramos[1]
Fernando Quintana[2]
Consuelo Díez[2]
Carlos Leno[1]
José Berciano[1]

Thirty-five CT scans were studied from patients with several forms of spinocerebellar degeneration. Atrophy was determined by objective measurements of the number and width of cerebellar sulci, transverse diameter and surface area of the fourth ventricle, brainstem ratio, cerebellopontine angle cistern, and Evans' index. Two-thirds of the patients with Friedreich's ataxia showed moderate cerebellar atrophy and an increase in the surface area of the fourth ventricle. Severe cerebellar atrophy and enlargement of the cerebellopontine angle cistern was seen in patients with olivopontocerebellar (OPC) atrophy and idiopathic cortical cerebellar atrophy. In the OPC atrophy group there was also prominent atrophy of the brainstem and an increase in the fourth ventricle parameters. Alcoholic cerebellar degeneration showed a specific pattern of cerebellar atrophy most prominent in the superior vermis, together with a slight increase in the fourth ventricle surface, a reduction in the size of the brainstem, and an enlargement of the cerebellopontine angle cistern. Supratentorial atrophy was present only in the OPC and alcoholic atrophy groups. In one patient with spastic ataxia, CT was normal but MR imaging revealed prominent atrophy of the spinal cord. These CT patterns appear to be distinctive enough to permit the diagnosis and classification of the various forms of spinocerebellar degeneration.

Spinocerebellar degeneration comprises a heterogeneous group of progressive diseases characterized by ataxia and spinocerebellar degeneration [1]. The diagnosis is based on clinical features, the pattern of genetic transmission, and electrophysiologic and neuroradiologic findings [2, 3]. CT has become important in evaluating spinocerebellar degeneration as it affords delineation of the atrophic structures [4–15]. We evaluated the CT findings in patients with the diagnosis of spinocerebellar degeneration including alcoholic cerebellar degeneration.

Subjects and Methods

Twelve women and 23 men with spinocerebellar degeneration were examined. Eleven patients 11–56 years old (mean, 32) had Friedreich's ataxia according to the clinical criteria of Harding [2]. Eleven patients 38–73 years old (mean, 54.7) had late-onset ataxia together with rigidity, chorea, pyramidal signs, dysphagia, ophthalmoplegia, dementia, sensory loss, amyotrophy, or sphincter disturbances. Presumptive clinical diagnosis was olivopontocerebellar (OPC) atrophy [2, 3, 16], hereditary (Menzel-type) in two patients and sporadic (Dejerine-Thomas–type) in nine. Six patients 50–74 years old (mean, 60) had pure cerebellar syndrome with late onset. Presumptive clinical diagnosis was idiopathic cortical cerebellar atrophy [2]. Six patients 30–59 years old (mean, 49.6) had alcoholic cerebellar degeneration. One 40-year-old man had hereditary spastic ataxia with no other clinical manifestations. Presumptive clinical diagnosis was predominantly spinal (Sanger-Brown) ataxia [1].

Thirty-six CT scans were used as controls from patients who had normal neurologic examinations. These patients were 21–71 years old (mean, 50.2).

The scans were obtained with a GE 8800 scanner with a 360 × 360 matrix. In accordance with Koller et al. [11], atrophy of vermian structures was diagnosed when two or more sulci were seen and atrophy of the cerebellar hemispheres if hemispheric sulci were visible. The

number of hemispheric and vermian sulci and their medium width were also determined. Measurements were made of the maximum width and surface area of the fourth ventricle. The relative size of the brainstem was expressed as a ratio of the width of the prepontine cistern divided by the distance between the posterior clinoid and the fourth ventricle [11]. These distances and area were measured with a CT cursor and expressed in actual values. Sections 5 mm thick and passing through the dorsum sellae and lateral recesses of the fourth ventricle were used to study the brainstem parameters. If this cut was not available, reconstructions were made including these structures. The cerebellopontine angle cistern was measured directly from the films and converted to actual distance by using the CT scale

provided. In each diagnostic category we established the percentage of cases in which the cerebellar lateral cistern was seen.

It has been stated that there is a poor correlation between the degree of atrophy observed on CT images and the degree of mental deterioration [17–19]. Our assessment of cerebral cortex atrophy was made exclusively by using the Evans' index [20]. Statistical analysis was performed with Student's t test and Fisher's exact test.

Results

The brainstem parameters are listed in Table 1.

TABLE 1: Measurements of Brainstem Parameters and Cerebellar Sulci in Spinocerebellar Degeneration

Parameter	Clinical Group (Mean Values ± SD)				
	Controls ($n = 36$)	Friedreich's Ataxia ($n = 11$)	Olivoponto-cerebellar Atrophy ($n = 11$)	Cortical Cerebellar Atrophy ($n = 6$)	Alcoholic Degeneration ($n = 6$)
Fourth ventricle:					
Transverse diameter (cm)	1.44 ± 0.22	1.62 ± 0.53	1.69 ± 0.44[a]	1.46 ± 0.47	1.51 ± 0.15
Surface area (cm²)	0.83 ± 0.26	1.22 ± 0.47[b]	1.85 ± 0.54[c]	0.85 ± 0.5	1.09 ± 0.22[a]
Brainstem ratio	0.23 ± 0.04	0.27 ± 0.1	0.38 ± 0.07[c]	0.23 ± 0.07	0.30 ± 0.04[b]
Cerebellopontine angle cistern (mm)	3.12 ± 0.56	3.11 ± 0.96	5.86 ± 0.65[c]	4.24 ± 0.82[b]	4.35 ± 0.62[c]
Cerebellar sulci:					
No. in hemispheres	0	1.64 ± 2.16[c]	7.64 ± 2.73[c]	5.67 ± 1.37[c]	2.83 ± 2.14[c]
No. in vermis	0.62 ± 0.8	1.18 ± 1.47	5.45 ± 2.34[c]	5.67 ± 1.97[c]	4.17 ± 0.75[c]
Width in hemispheres (mm)	. . .	1.44 ± 0.8[c]	2.29 ± 0.47[c]	1.80 ± 0.57[c]	1.62 ± 0.4[c]
Width in vermis (mm)	0.9 ± 0	1.62 ± 0.4[c]	2.37 ± 0.45[c]	2.25 ± 0.75[c]	2.25 ± 0.49[c]

Note.—Atrophy of cerebellar sulci was diagnosed when two or more sulci were seen; in 92% of cases there was no vermian atrophy. In 55% of cases there was no hemispheric atrophy (no sulci were seen).

[a] Differs from controls ($p < .05$).

[b] Differs from controls ($p < .005$).
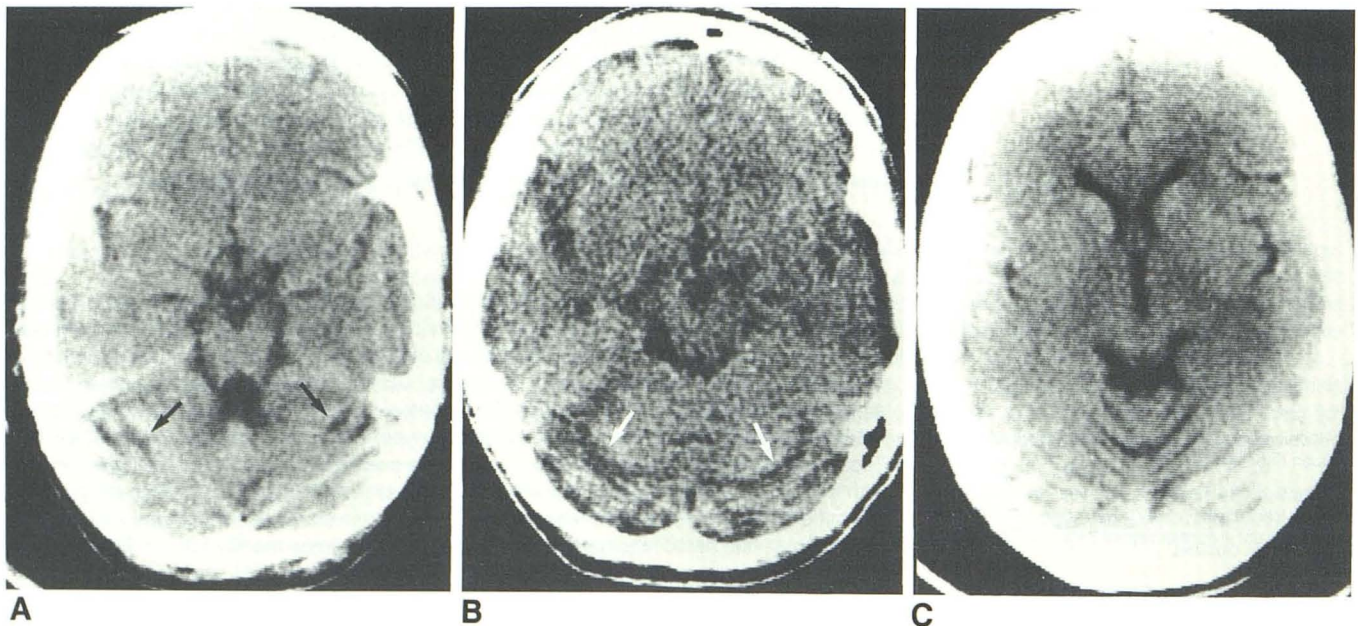
[c] Differs from controls ($p < .001$).

Fig. 1.—Friedreich's ataxia in two patients. CT shows enlargement of fourth ventricle (A), hemispheric atrophy (arrows, A and B), and vermian atrophy (C).

Fourth Ventricle

The transverse diameter of the fourth ventricle was significantly greater in the OPC atrophy group than in normal controls (Figs. 1–5). By contrast, the surface area was greater in all types of spinocerebellar degeneration, except cortical cerebellar atrophy. The surface areas in OPC atrophy were significantly greater than those in Friedreich's ataxia ($p <$ .025) and alcoholic degeneration ($p <$ .01).

Brainstem Ratios

The brainstem ratio was increased in OPC atrophy and alcoholic cerebellar degeneration (Figs. 2, 3, and 5). The

difference between the two values was statistically significant ($p <$ .025).

Cerebellopontine Angle Cistern

This cistern was enlarged in all our diagnostic categories except in Friedreich's ataxia (Figs. 2–5). In the OPC atrophy group the values were greater than those of cortical cerebellar atrophy and alcoholic degeneration ($p <$ .001).

Cerebellar Atrophy

In the control group hemispheric atrophy did not occur, but 8% of the patients had vermian atrophy, and the lateral cistern
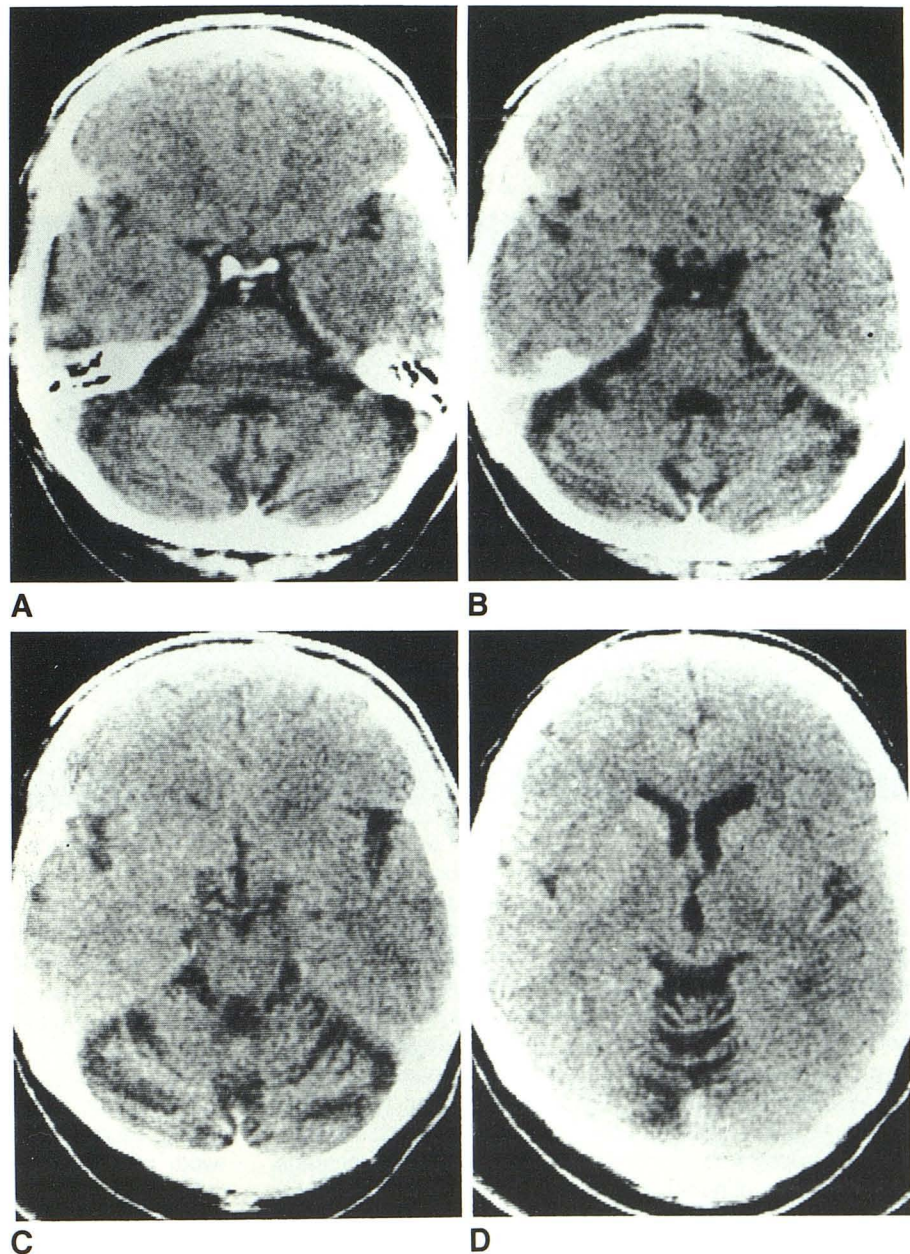

Fig. 2.—Dominant olivopontocerebellar atrophy. CT shows enlargement of fourth ventricle and lateral cerebellar, prepontine, and cerebellopontine cisterns (*A–C*), together with severe enlargement of hemispheric (*C*) and vermian (*D*) sulci.
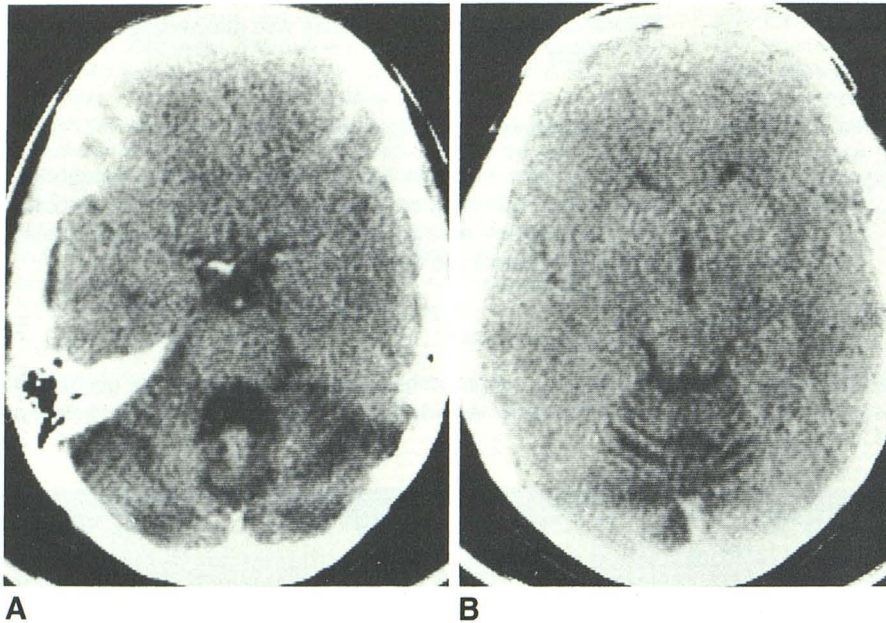
Fig. 3.—Sporadic olivopontocerebellar atrophy. CT shows marked enlargement of fourth ventricle and prepontine cistern (A) combined with hemispheric (A) and vermian (B) atrophy.
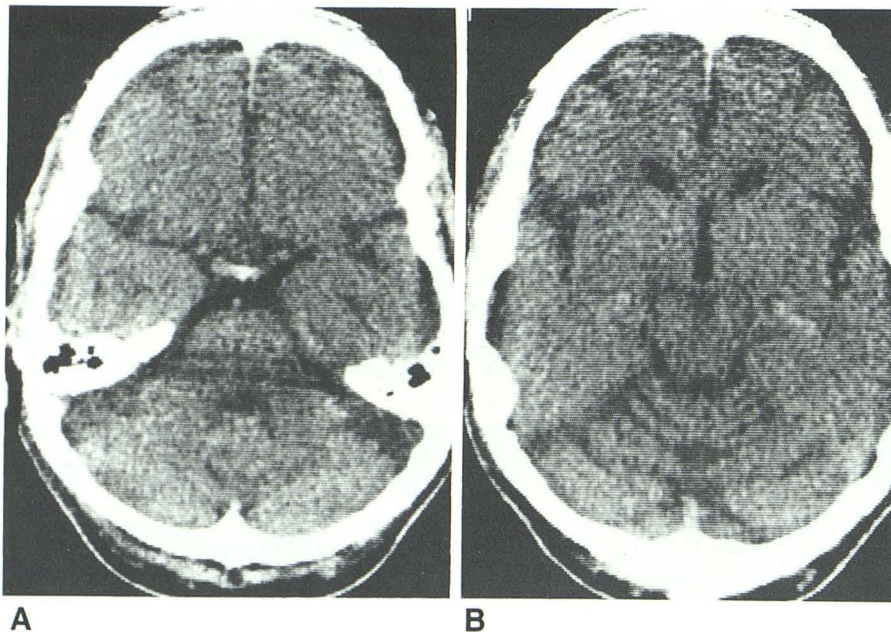

Fig. 4.—Cortical cerebellar atrophy. CT shows enlargement of lateral cerebellar and cerebello-pontine cisterns (A) combined with vermian and hemispheric (B) atrophy.
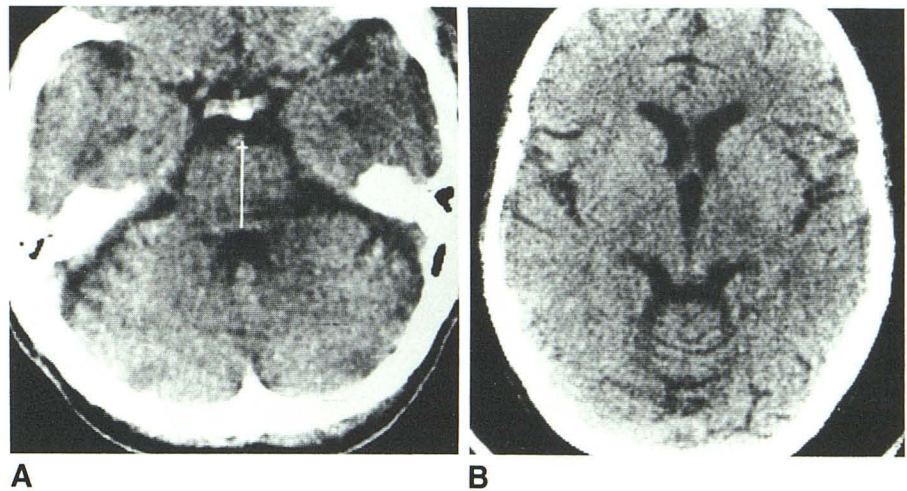
was seen in 12% of cases. The percentages of hemispheric atrophy were 45% for Friedreich's ataxia, 83% for alcoholic cerebellar degeneration, and 100% for OPC and cortical cerebellar atrophy (Figs. 1–5); the difference from the control group was significant ($p < .001$). Vermian atrophy (Figs. 1–5) was constant in OPC atrophy, cortical cerebellar atrophy, and alcoholic degeneration; the difference from the control group was also significant ($p < .001$). In Friedreich's ataxia, vermian atrophy was observed in 36% of cases, a percentage not statistically different from the control group. The lateral cisterns were seen in 9% of patients with Friedreich's ataxia,

in 91% with OPC atrophy ($p < .001$), and in 67% with cortical cerebellar atrophy and alcoholic cerebellar degeneration ($p < .01$).

Cerebellar Sulci

Except for the number of vermian sulci in Friedreich's ataxia, there was a significant increase in the number and width of the cerebellar and vermian sulci in all diagnostic categories (Table 1). In comparison with Friedreich's ataxia and alcoholic cerebellar degeneration, patients with OPC

A   B

atrophy and cortical cerebellar atrophy had a greater number of hemispheric sulci ($p < .01$). There was less widening of vermian sulci in Friedreich's ataxia than in the other groups ($p < .01$). Finally, patients with OPC atrophy had the widest hemispheric sulci, the difference being significant from the Friedreich's ataxia and alcoholic degeneration groups ($p < .005$) and from the cortical cerebellar atrophy group ($p < .05$).

Evans' Index

This index was significantly greater in OPC atrophy ($p < .001$) and alcoholic cerebellar degeneration ($p < .01$) than in controls. In the patient with spastic ataxia no abnormalities were found on CT scan; nevertheless, MR imaging revealed significant atrophy of the spinal cord (Fig. 6).

Discussion

The CT signs observed in our study of the heredoataxias provide several CT patterns distinctive enough to be of value in the diagnosis and classification of these disorders when combined with clinical findings.

In agreement with other studies [7–10], one-third of our patients with Friedreich's ataxia had a normal CT scan. The course of the disease was 5–26 years, suggesting that CT findings can be normal even after an illness of long duration. The anatomic changes in this disease are chiefly localized in the spinal cord [1, 21, 22], so the absence of radiologic findings in the posterior fossa structures is not surprising.

In our other cases of Friedreich's ataxia, the significant signs were an increase in the surface area of the fourth ventricle and an enlargement of the hemispheric and vermian cerebellar sulci. An increase in the area of the fourth ventricle with normal width has not been reported previously. In our series, it may have resulted from atrophy of the dentate nuclei with degeneration of the efferent fibers, as is found frequently in Friedreich's ataxia, together with no involvement of the pontine nuclei and middle cerebellar peduncles [21, 22]. Whereas other studies [8, 10] have described cerebellar atrophy predominantly in the superior vermis, the hemi-

spheres and vermis were affected equally in our patients. This correlates with the loss of Purkinje cells, which sometimes are numerous in the vermis.

All our cases with suspected OPC atrophy had abnormal CT images [4, 9, 10, 13, 15]. Also in this category we found the highest incidence of abnormalities in all the parameters studied, with the exception of the Evans' index. A widened fourth ventricle occurred exclusively in OPC atrophy. In contrast, the surface area of the fourth ventricle was increased in OPC atrophy, Friedreich's ataxia, and alcoholic degeneration. Other authors [9, 10, 15] have reported an increase in the diameters of the fourth ventricle; however, its surface had not been measured in spinocerebellar degeneration. In our series, alterations in the brainstem ratio were detected only in OPC atrophy and alcoholic degeneration, which contradicts Koller et al. [11], who found the brainstem ratio to be significantly greater in the four groups of patients than in controls. The cerebellopontine angle cistern was enlarged in all our patients except in those with Friedreich's ataxia. Similar findings have been reported in OPC atrophy [9, 15], cortical cerebellar atrophy [9], and chronic alcoholism [11]. These CT changes further indicate that degeneration of the pontine nuclei and middle cerebellar peduncles are outstanding factors in enlargement of the fourth ventricle and cerebellopontine angle cistern and in atrophy of the brainstem. Another constant feature in our patients with OPC atrophy was severe pancerebellar wasting slightly more pronounced in the hemispheres [13], together with visualization of the lateral cerebellar cistern. Patients with OPC atrophy had a significant increase in the width of the hemispheric sulci compared with patients with cortical cerebellar atrophy and alcoholic cerebellar degeneration, and a greater number of these sulci were seen compared with the alcoholic group.

In agreement with pathologic studies [1, 22], our patients with idiopathic cortical cerebellar atrophy showed atrophy affecting the entire cerebellum and significant enlargement of the cerebellopontine angle cisterns.

In patients with alcoholic cerebellar degeneration CT revealed vermian and to a lesser extent hemispheric atrophy
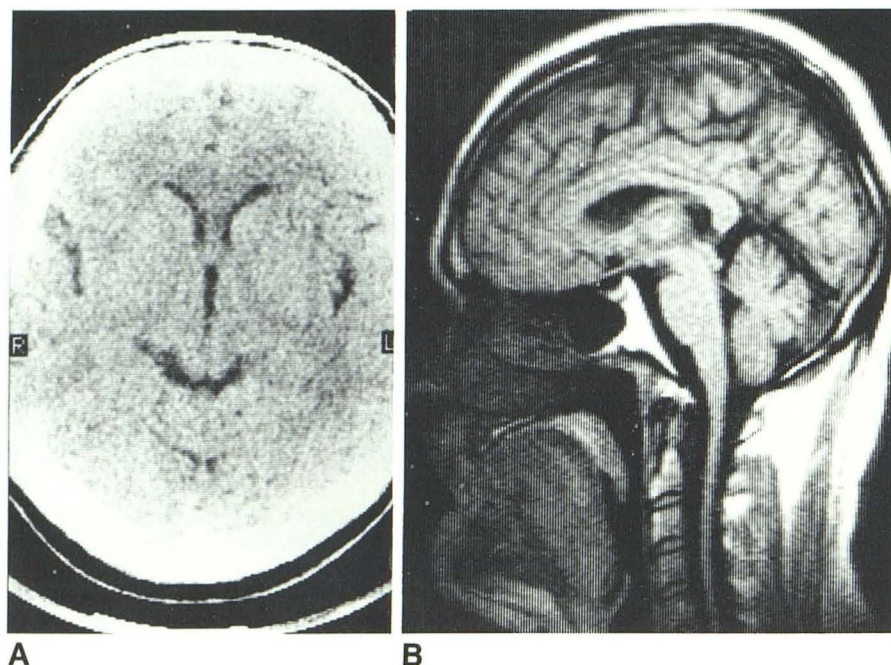
A   B

Fig. 6.—Hereditary spastic ataxia.
A, CT scan is normal.
B, MR shows uniform narrowing of spinal cord.

[7, 10, 11]. In addition, the cerebellopontine angle cistern, brainstem ratio, fourth ventricle surface, and Evans' index were significantly increased. These findings coincide partially with those reported by Koller et al. [11] and can be attributed to the diffuse toxic effect of alcohol on the central nervous system [23].

CT findings were normal in our patient with hereditary spastic ataxia. By contrast MR revealed a clear reduction in the diameter of the spinal cord. These findings suggest that MR can be the elective neuroimaging technique in the evaluation of the spinal forms of hereditary ataxias.

REFERENCES

1. Greenfield JG. The spinocerebellar degeneration. Oxford: Blackwell, 1954
2. Harding AE. The hereditary ataxias and related disorders. Edinburgh: Churchill Livingstone, 1984
3. Plaitakis A, Guddesblatt M. The hereditary ataxias. In: Appel SH, ed. Current neurology, vol 5. Chicago: Year Book, 1984:471–509
4. Aita JF. Cranial computerized tomography and Marie's ataxia. Arch Neurol 1978;35:55–56
5. Rothman SLG, Glanz S. Cerebellar atrophy: the differential diagnosis by computerized tomography. Neuroradiology 1978;16:123–126
6. Gyldensted C, Pedersen L. Computed tomography in hereditary ataxias. Neuroradiology 1978;16:327–328
7. Allen JH, Martin JT, McLain LW. Computed tomography in cerebellar atrophic processes. Radiology 1979;130:379–382
8. Langelier R, Bouchard JP, Bouchard R. Computed tomography of posterior fossa in hereditary ataxias. Can J Neurol Sci 1979;6:195–198
9. Maruyama S, Okayama K, Aikawa T, Saito Y, Kobayashi N. CT scan study of spinocerebellar degeneration. In: Sobue I, ed. Spinocerebellar degenerations. Tokyo: Tokyo University Press, 1980:60–82
10. Claus D, Aschoff JC. Cranial computerized tomography in spinocerebellar atrophies. Ann NY Acad Sci 1981;374:831–838
11. Koller WC, Glatt SN, Perlik S, Huckman MS, Fox JH. Cerebellar atrophy demonstrated by computed tomography. Neurology 1981;31:405–412
12. Huckman MS. Computed tomography in the diagnosis of degenerative brain disease. Radiol Clin North Am 1982;20:169–183
13. Savoiardo M, Bracchi M, Passerini A, Visciani A, Di Donato S, Cocchini F. CT of olivopontocerebellar degeneration. AJNR 1983;4:509–512
14. Andreula CF, Camicia M, Lorusso A, et al. Clinical and CT parameters in degenerative cerebellar atrophy. Neuroradiology 1984;26:29–30
15. Huang YP, Plaitakis A. Morphological changes of olivopontocerebellar atrophy in computed tomography and comments on its pathogenesis. In: Duvoisin RC, Plaitakis A, eds. The olivopontocerebellar atrophies. New York: Raven, 1984:39–85
16. Berciano J. Olivopontocerebellar atrophy. A review of 117 cases. J Neurol Sci 1982;53:253–272
17. Gado M, Hughes CH, Danziger W, Chi D, Jost G, Berg L. Volumetric measurements of the cerebrospinal fluid spaces in demented subjects and controls. Radiology 1982;144:535–538
18. Turkheimer E, Cullum CM, Hubler DW, Paver SW, Ayeo R, Bigler E. Quantifying cortical atrophy. J Neurol Neurosurg Psychiatry 1985;47:1314–1318
19. Yerby MS, Sundsten JW, Larson EB, Wu SA, Sumi SN. A new method of measuring brain atrophy. Neurology 1985;35:1316–1320
20. Meese W, Kluge W, Grumme T, Hopfenmüller W. CT evaluation of the CSF spaces of healthy persons. Neuroradiology 1980;19:131–136
21. Lamarche JB, Lemieux B, Lieu HB. The neuropathology of "typical" Friedreich's ataxia in Quebec. Can J Neurol Sci 1984;11:592–600
22. Oppenheimer DR. Diseases of the basal ganglia, cerebellum and motor neurons. In: Adams JH, Corsellis JAN, Duchen LW, eds. Greenfield's neuropathology. London: Edward Arnold, 1984:699–747
23. Harper CG, Krill JJ, Holloway RL. Brain shrinkage in chronic alcoholics: a pathological study. Br Med J [Clin Res] 1985;290:501–504